2014年9月2日

論文紹介2014秋

コンプトン散乱による異方性探査／量子イメージング

道村唯太

東京大学 大学院理学系研究科 物理学専攻

安東研究室

博士論文現状

- Abstract (要旨)
- 1. Introduction (序論)
- 2. Tests of Lorentz Invariance (理論、先行研究)
- 3. Optical Ring Cavity (原理)
- 4. Experimental Setup (装置)
- 5. Data Analysis (解析)
- 6. Conclusion (結論)
- A. Standard Model Extension (解析)
- B. C. D. E. Feedback Control etc. (補足説明)
- Acknowledgements (謝辞)

球面調和関数展開

- SMEでは実験の精度がわかりにくいので、異方性を球面調和関数展開し、その係数に上限値
- SMEは補遺に回す

$$Y_l^m(\theta,\phi) = (-1)^m \sqrt{\frac{2l+1}{4\pi}\frac{(l-m)!}{(l+m)!}} P_l^m(\cos\theta) e^{im\phi}, \tag{2.15}$$

the speed of light can be expanded as

$$c(\theta,\phi) = 1 + \sum_{l=0}^{\infty}\sum_{m=0}^{l} \mathrm{Re}\left[(\overline{y}_l^m)^* Y_l^m(\theta,\phi)\right]. \tag{2.16}$$

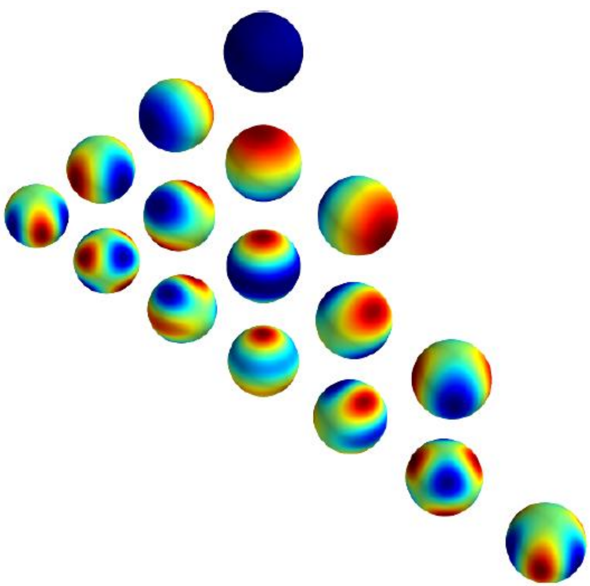

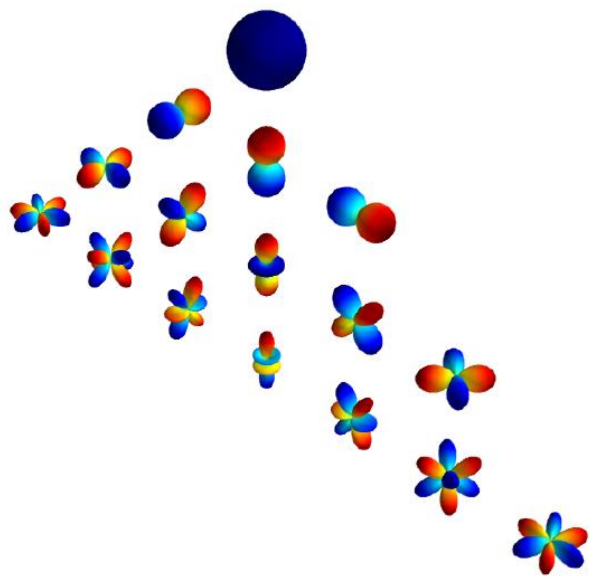

座標変換

- SCCEF(太陽中心系)で考える
  CMB静止系に対して一定速度のため、
  異方性も実験期間中一定と考えられる

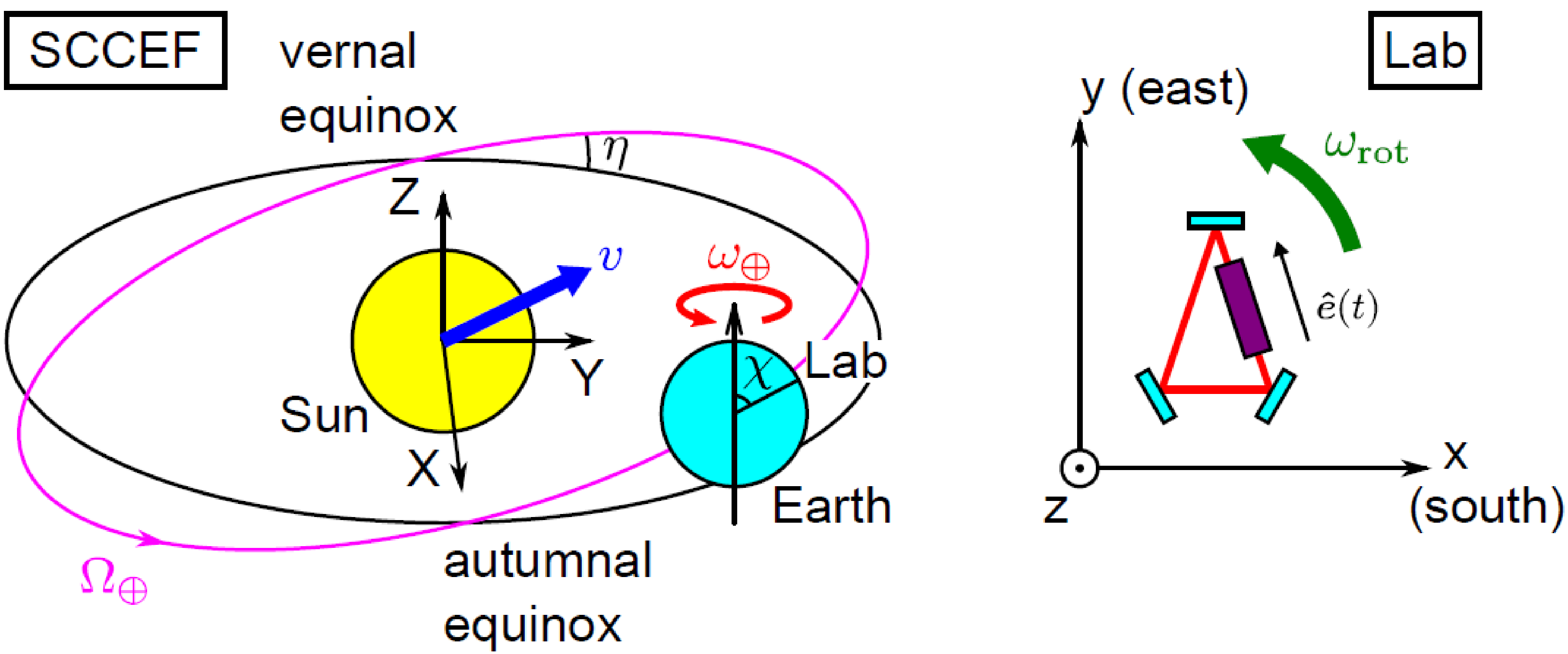

Figure 5.1: SCCEF and the laboratory frame

装置の回転と地球の自転

- 装置の回転では180度回転で共振周波数差を反転させる
  - l=奇数にしか感度がない
- 地球の自転では180度回転で完全な反転にはならない
  - m=偶数にも感度がある
- l=1,3とm=0,1,2,3を考える

球面調和関数 $l = 1$ [編集]

$$Y_1^{-1}(x) = \frac{1}{2}\sqrt{\frac{3}{2\pi}} \cdot e^{-i\varphi} \cdot \sin\theta \quad = \frac{1}{2}\sqrt{\frac{3}{2\pi}} \cdot \frac{(x - iy)}{r}$$

$$Y_1^{0}(x) = \frac{1}{2}\sqrt{\frac{3}{\pi}} \cdot \cos\theta \quad = \frac{1}{2}\sqrt{\frac{3}{\pi}} \cdot \frac{z}{r}$$

$$Y_1^{1}(x) = \frac{-1}{2}\sqrt{\frac{3}{2\pi}} \cdot e^{i\varphi} \cdot \sin\theta \quad = \frac{-1}{2}\sqrt{\frac{3}{2\pi}} \cdot \frac{(x + iy)}{r}$$

球面調和関数 $l = 2$ [編集]

$$Y_2^{-2}(x) = \frac{1}{4}\sqrt{\frac{15}{2\pi}} \cdot e^{-2i\varphi} \cdot \sin^2\theta \quad = \frac{1}{4}\sqrt{\frac{15}{2\pi}} \cdot \frac{(x^2 - 2ixy - y^2)}{r^2}$$

$$Y_2^{-1}(x) = \frac{1}{2}\sqrt{\frac{15}{2\pi}} \cdot e^{-i\varphi} \cdot \sin\theta \cdot \cos\theta \quad = \frac{1}{2}\sqrt{\frac{15}{2\pi}} \cdot \frac{(xz - iyz)}{r^2}$$

$$Y_2^{0}(x) = \frac{1}{4}\sqrt{\frac{5}{\pi}} \cdot (3\cos^2\theta - 1) \quad = \frac{1}{4}\sqrt{\frac{5}{\pi}} \cdot \frac{(-x^2 - y^2 + 2z^2)}{r^2}$$

$$Y_2^{1}(x) = \frac{-1}{2}\sqrt{\frac{15}{2\pi}} \cdot e^{i\varphi} \cdot \sin\theta \cdot \cos\theta \quad = \frac{-1}{2}\sqrt{\frac{15}{2\pi}} \cdot \frac{(xz + iyz)}{r^2}$$

$$Y_2^{2}(x) = \frac{1}{4}\sqrt{\frac{15}{2\pi}} \cdot e^{2i\varphi} \cdot \sin^2\theta \quad = \frac{1}{4}\sqrt{\frac{15}{2\pi}} \cdot \frac{(x^2 + 2ixy - y^2)}{r^2}$$

球面調和関数 $l = 3$ [編集]

$$Y_3^{-3}(x) = \frac{1}{8}\sqrt{\frac{35}{\pi}} \cdot e^{-3i\varphi} \cdot \sin^3\theta \quad = \frac{1}{8}\sqrt{\frac{35}{\pi}} \cdot \frac{(x^3 - 3ix^2y - 3xy^2 + iy^3)}{r^3}$$

$$Y_3^{-2}(x) = \frac{1}{4}\sqrt{\frac{105}{2\pi}} \cdot e^{-2i\varphi} \cdot \sin^2\theta \cdot \cos\theta \quad = \frac{1}{4}\sqrt{\frac{105}{2\pi}} \cdot \frac{(x^2z - 2ixyz - y^2z)}{r^3}$$

$$Y_3^{-1}(x) = \frac{1}{8}\sqrt{\frac{21}{\pi}} \cdot e^{-i\varphi} \cdot \sin\theta \cdot (5\cos^2\theta - 1) \quad = \frac{1}{8}\sqrt{\frac{21}{\pi}} \cdot \frac{(-x^3 + ix^2y - xy^2 + 4xz^2 + iy^3 - 4iyz^2)}{r^3}$$

$$Y_3^{0}(x) = \frac{1}{4}\sqrt{\frac{7}{\pi}} \cdot (5\cos^3\theta - 3\cos\theta) \quad = \frac{1}{4}\sqrt{\frac{7}{\pi}} \cdot \frac{(-3x^2z - 3y^2z + 2z^3)}{r^3}$$

$$Y_3^{1}(x) = \frac{-1}{8}\sqrt{\frac{21}{\pi}} \cdot e^{i\varphi} \cdot \sin\theta \cdot (5\cos^2\theta - 1) \quad = \frac{-1}{8}\sqrt{\frac{21}{\pi}} \cdot \frac{(-x^3 - ix^2y - xy^2 + 4xz^2 - iy^3 + 4iyz^2)}{r^3}$$

$$Y_3^{2}(x) = \frac{1}{4}\sqrt{\frac{105}{2\pi}} \cdot e^{2i\varphi} \cdot \sin^2\theta \cdot \cos\theta \quad = \frac{1}{4}\sqrt{\frac{105}{2\pi}} \cdot \frac{(x^2z + 2ixyz - y^2z)}{r^3}$$

$$Y_3^{3}(x) = \frac{-1}{8}\sqrt{\frac{35}{\pi}} \cdot e^{3i\varphi} \cdot \sin^3\theta \quad = \frac{-1}{8}\sqrt{\frac{35}{\pi}} \cdot \frac{(x^3 + 3ix^2y - 3xy^2 - iy^3)}{r^3}$$

http://ja.wikipedia.org/wiki/球面調和関数表

復調

- まずテーブルの回転周波数で復調(1,3)

$$\frac{\delta\nu}{\nu} = \sum_{m_{\rm r}>0} \left[C_{m_{\rm r}} \cos\left(m_{\rm r}\omega_{\rm rot}t\right) + S_{m_{\rm r}} \sin\left(m_{\rm r}\omega_{\rm rot}t\right)\right]. \qquad (5.22)$$

- 次に地球自転周波数で復調(0,1,2,3)

$$C_{m_{\rm r}} = \sum_{m_\oplus \geq 0} \left[C^C_{m_{\rm r}m_\oplus} \cos\left(m_\oplus \omega_\oplus T_\oplus\right) + C^S_{m_{\rm r}m_\oplus} \sin\left(m_\oplus \omega_\oplus T_\oplus\right)\right], \quad (5.23)$$

$$S_{m_{\rm r}} = \sum_{m_\oplus \geq 0} \left[S^C_{m_{\rm r}m_\oplus} \cos\left(m_\oplus \omega_\oplus T_\oplus\right) + S^S_{m_{\rm r}m_\oplus} \sin\left(m_\oplus \omega_\oplus T_\oplus\right)\right]. \quad (5.24)$$

復調振幅と係数

- Imとの対応がわかりやすい

$m_{\rm r}$	$m_\oplus$	$C^C_{m_{\rm r}m_\oplus}$	$C^S_{m_{\rm r}m_\oplus}$	$S^C_{m_{\rm r}m_\oplus}$	$S^S_{m_{\rm r}m_\oplus}$
1	0	$-0.22\ \overline{y}^0_1$	-	0	-
		$+0.089\ \overline{y}^0_3$			
1	1	$0.11{\rm Re}[\overline{y}^1_1]$	$0.11{\rm Im}[\overline{y}^1_1]$	$0.19{\rm Im}[\overline{y}^1_1]$	$-0.19{\rm Re}[\overline{y}^1_1]$
		$+0.16{\rm Re}[\overline{y}^1_3]$	$+0.16{\rm Im}[\overline{y}^1_3]$	$-0.032{\rm Im}[\overline{y}^1_3]$	$+0.032{\rm Re}[\overline{y}^1_3]$
1	2	$-0.0025{\rm Re}[\overline{y}^2_3]$	$-0.0025{\rm Im}[\overline{y}^2_3]$	$-0.14{\rm Im}[\overline{y}^2_3]$	$0.14{\rm Re}[\overline{y}^2_3]$
1	3	$-0.067{\rm Re}[\overline{y}^3_3]$	$-0.067{\rm Im}[\overline{y}^3_3]$	$-0.12{\rm Im}[\overline{y}^3_3]$	$0.12{\rm Re}[\overline{y}^3_3]$
3	0	$-0.17\ \overline{y}^0_3$	-	$0.18\ \overline{y}^0_3$	-
3	1	$0.10{\rm Re}[\overline{y}^1_3]$	$-0.19{\rm Re}[\overline{y}^1_3]$	$-0.11{\rm Re}[\overline{y}^1_3]$	$-0.18{\rm Re}[\overline{y}^1_3]$
		$+0.19{\rm Im}[\overline{y}^1_3]$	$+0.10{\rm Im}[\overline{y}^1_3]$	$0.18{\rm Im}[\overline{y}^1_3]$	$-0.11{\rm Im}[\overline{y}^1_3]$
3	2	$-0.19{\rm Re}[\overline{y}^2_3]$	$0.17{\rm Re}[\overline{y}^2_3]$	$0.20{\rm Re}[\overline{y}^2_3]$	$0.16{\rm Re}[\overline{y}^2_3]$
		$-0.17{\rm Im}[\overline{y}^2_3]$	$-0.19{\rm Im}[\overline{y}^2_3]$	$-0.16{\rm Im}[\overline{y}^2_3]$	$0.20{\rm Im}[\overline{y}^2_3]$
3	3	$0.14{\rm Re}[\overline{y}^3_3]$	$-0.15{\rm Re}[\overline{y}^3_3]$	$-0.14{\rm Re}[\overline{y}^3_3]$	$-0.14{\rm Re}[\overline{y}^3_3]$
		$+0.15{\rm Im}[\overline{y}^3_3]$	$+0.14{\rm Im}[\overline{y}^3_3]$	$+0.14{\rm Im}[\overline{y}^3_3]$	$-0.14{\rm Im}[\overline{y}^3_3]$

得られた上限値

- SMEと同じ構造

m_r	$m_\oplus$	$C^C_{m_r m_\oplus}$	$C^S_{m_r m_\oplus}$	$S^C_{m_r m_\oplus}$	$S^S_{m_r m_\oplus}$
1	0	-0.1 ± 1.0	-	0.2 ± 1.0	-
1	1	-0.6 ± 1.4	-1.2 ± 1.4	-0.3 ± 1.4	1.0 ± 1.4
1	2	-0.9 ± 1.4	-0.2 ± 1.4	-0.1 ± 1.4	1.0 ± 1.4
1	3	-0.8 ± 1.4	0.2 ± 1.4	-0.5 ± 1.4	0.6 ± 1.4
3	0	0.12 ± 0.46	-	0.15 ± 0.46	-
3	1	-0.79 ± 0.64	-1.1 ± 0.65	-0.48 ± 0.64	-0.51 ± 0.65
3	2	-1.1 ± 0.65	0.57 ± 0.65	-0.46 ± 0.65	0.21 ± 0.65
3	3	0.40 ± 0.65	0.16 ± 0.65	-0.36 ± 0.64	0.75 ± 0.65

Dimension	Coefficient	Measurement
$d=6$	$(\overline{c}^{(6)}_F)^{(0E)}_{110}$	$(-0.1 \pm 1.5) \times 10^3$ GeV^{-2}
	$\mathrm{Re}[(\overline{c}^{(6)}_F)^{(0E)}_{111}]$	$(-0.8 \pm 1.1) \times 10^3$ GeV^{-2}
	$\mathrm{Im}[(\overline{c}^{(6)}_F)^{(0E)}_{111}]$	$(-0.6 \pm 1.0) \times 10^3$ GeV^{-2}
$d=8$	$-0.020(\overline{c}^{(8)}_F)^{(0E)}_{110} + (\overline{c}^{(8)}_F)^{(0E)}_{310}$	$(-0.2 \pm 1.9) \times 10^{19}$ GeV^{-4}
	$\mathrm{Re}[-0.020(\overline{c}^{(8)}_F)^{(0E)}_{111} + (\overline{c}^{(8)}_F)^{(0E)}_{311}]$	$(1.4 \pm 1.3) \times 10^{19}$ GeV^{-4}
	$\mathrm{Re}[-0.020(\overline{c}^{(8)}_F)^{(0E)}_{111} + (\overline{c}^{(8)}_F)^{(0E)}_{311}]$	$(0.1 \pm 1.3) \times 10^{19}$ GeV^{-4}
	$(\overline{c}^{(8)}_F)^{(0E)}_{330}$	$(-0.8 \pm 3.3) \times 10^{19}$ GeV^{-4}
	$\mathrm{Re}[(\overline{c}^{(8)}_F)^{(0E)}_{331}]$	$(-0.3 \pm 1.9) \times 10^{19}$ GeV^{-4}
	$\mathrm{Im}[(\overline{c}^{(8)}_F)^{(0E)}_{331}]$	$(-2.8 \pm 1.9) \times 10^{19}$ GeV^{-4}
	$\mathrm{Re}[(\overline{c}^{(8)}_F)^{(0E)}_{332}]$	$(2.2 \pm 1.3) \times 10^{19}$ GeV^{-4}
	$\mathrm{Im}[(\overline{c}^{(8)}_F)^{(0E)}_{332}]$	$(0.2 \pm 1.3) \times 10^{19}$ GeV^{-4}
	$\mathrm{Re}[(\overline{c}^{(8)}_F)^{(0E)}_{333}]$	$(-0.1 \pm 1.6) \times 10^{19}$ GeV^{-4}
	$\mathrm{Im}[(\overline{c}^{(8)}_F)^{(0E)}_{333}]$	$(-0.1 \pm 1.6) \times 10^{19}$ GeV^{-4}

Coefficient	Measurement
$\overline{y}^0_1$	0.4 ± 4.4
$\mathrm{Re}[\overline{y}^1_1]$	-5.7 ± 6.3
$\mathrm{Im}[\overline{y}^1_1]$	-3.2 ± 6.2
$\overline{y}^0_3$	0.1 ± 1.9
$\mathrm{Re}[\overline{y}^1_3]$	2.9 ± 2.2
$\mathrm{Im}[\overline{y}^1_3]$	-3.2 ± 2.1
$\mathrm{Re}[\overline{y}^2_3]$	2.1 ± 1.8
$\mathrm{Im}[\overline{y}^2_3]$	1.5 ± 1.8
$\mathrm{Re}[\overline{y}^3_3]$	-0.2 ± 2.2
$\mathrm{Im}[\overline{y}^3_3]$	-0.7 ± 2.2

単位は10^{-15}

コンプトン散乱による異方性探査

- J.-P. Bocquet et al.: [PRL 104, 241601 (2010)]
- 片道光速の異方性に1.4×10^{-14}の上限値がつけられている (我々は6×10^{-15})
- メール、CPT'13で著者に指摘されるまで認識してなかった

PRL **104,** 241601 (2010) PHYSICAL REVIEW LETTERS week ending 18 JUNE 2010

Limits on Light-Speed Anisotropies from Compton Scattering of High-Energy Electrons

J.-P. Bocquet,[1] D. Moricciani,[2] V. Bellini,[3] M. Beretta,[4] L. Casano,[2] A. D'Angelo,[5] R. Di Salvo,[2] A. Fantini,[5] D. Franco,[5] G. Gervino,[6] F. Ghio,[7] G. Giardina,[8] B. Girolami,[7] A. Giusa,[3] V. G. Gurzadyan,[9,10] A. Kashin,[9] S. Knyazyan,[9] A. Lapik,[11] R. Lehnert,[12,*] P. Levi Sandri,[4] A. Lleres,[1] F. Mammoliti,[3] G. Mandaglio,[8] M. Manganaro,[8] A. Margarian,[9] S. Mehrabyan,[9] R. Messi,[5] V. Nedorezov,[11] C. Perrin,[1] C. Randieri,[3] D. Rebreyend,[1,†] N. Rudnev,[11] G. Russo,[3] C. Schaerf,[5] M. L. Sperduto,[3] M. C. Sutera,[3] A. Turinge,[11] and V. Vegna[5]

[1]*LPSC, UJF Grenoble 1, CNRS/IN2P3, INPG, 53 avenue des Martyrs 38026 Grenoble, France*
[2]*INFN Sezione di Roma TV, 00133 Roma, Italy*
[3]*INFN Sezione di Catania and Università di Catania, 95100 Catania, Italy*
[4]*INFN Laboratori Nazionali di Frascati, 00044 Frascati, Italy*
[5]*INFN Sezione di Roma TV and Università di Roma "Tor Vergata," 00133 Roma, Italy*
[6]*INFN Sezione di Torino and Università di Torino, 10125 Torino, Italy*
[7]*INFN Sezione di Roma I and Istituto Superiore di Sanità, 00161 Roma, Italy*
[8]*INFN Sezione di Catania and Università di Messina, 98166 Messina, Italy*
[9]*Yerevan Physics Institute, 375036 Yerevan, Armenia*
[10]*Yerevan State University, 375025 Yerevan, Armenia*
[11]*Institute for Nuclear Research, 117312 Moscow, Russia*
[12]*ICN, Universidad Nacional Autónoma de México, A. Postal 70-543, 04510 México D.F., Mexico*

(Received 22 February 2010; published 17 June 2010)

上限値の比較

- [107]が我々
- [108]が彼ら

Table D11. Photon sector, $d = 4$ (part 3 of 4)

Combination	Result	System	Ref.
$\tilde{\kappa}_{o+}^{XY}$	$(0.7 \pm 1.0) \times 10^{-14}$	Optical ring cavity	[107]
$(\tilde{\kappa}_{o+})^{XY}$	$(-1.5 \pm 1.2) \times 10^{-12}$	Rotating microwave resonators	[95]
$\sqrt{[2c_{TX} - (\tilde{\kappa}_{o+})^{YZ}]^2 + [2c_{TY} - (\tilde{\kappa}_{o+})^{ZX}]^2}$	$< 1.6 \times 10^{-14}$	Compton scattering	[108]
$\beta_{\oplus}(\tilde{\kappa}_{o+})^{XY}$	$(-0.14 \pm 0.78) \times 10^{-17}$	Rotating optical resonators	[96]
$(\tilde{\kappa}_{o+})^{XY}$	$(1.5 \pm 1.5 \pm 0.2) \times 10^{-13}$	"	[97]
$\beta_{\oplus}(\tilde{\kappa}_{o+})^{XY}$	$(-2.5 \pm 2.5) \times 10^{-17}$	"	[98]
$(\tilde{\kappa}_{o+})^{XY}$	$(1.7 \pm 2.0) \times 10^{-12}$	Optical, microwave resonators	[46]*
"	$(-0.9 \pm 2.6) \times 10^{-12}$	Rotating microwave resonators	[99]
"	$(-2.5 \pm 5.1) \times 10^{-12}$	Rotating optical resonators	[100]
"	$(0.20 \pm 0.21) \times 10^{-11}$	Rotating microwave resonators	[101]
"	$(-1.8 \pm 1.5) \times 10^{-11}$	Microwave resonator, maser	[102]
"	$(14 \pm 14) \times 10^{-11}$	Optical resonators	[103]
$\tilde{\kappa}_{o+}^{XZ}$	$(-0.6 \pm 1.2) \times 10^{-14}$	Optical ring cavity	[107]
$(\tilde{\kappa}_{o+})^{XZ}$	$(1.6 \pm 2.2) \times 10^{-13}$	Asymmetric optical resonator	[109]
"	$(0.7 \pm 1.4) \times 10^{-12}$	"	[110]
"	$(1.7 \pm 0.7) \times 10^{-12}$	Rotating microwave resonators	[95]
$\beta_{\oplus}(\tilde{\kappa}_{o+})^{XZ}$	$(-0.45 \pm 0.62) \times 10^{-17}$	Rotating optical resonators	[96]
$(\tilde{\kappa}_{o+})^{XZ}$	$(-0.1 \pm 1.0 \pm 0.2) \times 10^{-13}$	"	[97]
$\beta_{\oplus}(\tilde{\kappa}_{o+})^{XZ}$	$(1.5 \pm 1.7) \times 10^{-17}$	"	[98]
$(\tilde{\kappa}_{o+})^{XZ}$	$(-3.1 \pm 2.3) \times 10^{-12}$	Optical, microwave resonators	[46]*
"	$(-4.4 \pm 2.5) \times 10^{-12}$	Rotating microwave resonators	[99]
"	$(-3.6 \pm 2.7) \times 10^{-12}$	Rotating optical resonators	[100]
"	$(-0.91 \pm 0.46) \times 10^{-11}$	Rotating microwave resonators	[101]
"	$(-1.4 \pm 2.3) \times 10^{-11}$	Microwave resonator, maser	[102]
"	$(-1.2 \pm 2.6) \times 10^{-11}$	Optical resonators	[103]
$\tilde{\kappa}_{o+}^{YZ}$	$(0.5 \pm 1.0) \times 10^{-14}$	Optical ring cavity	[107]
$(\tilde{\kappa}_{o+})^{YZ}$	$(0.2 \pm 0.7) \times 10^{-12}$	Rotating microwave resonators	[95]
$\beta_{\oplus}(\tilde{\kappa}_{o+})^{YZ}$	$(-0.34 \pm 0.61) \times 10^{-17}$	Rotating optical resonators	[96]
$(\tilde{\kappa}_{o+})^{YZ}$	$(-0.1 \pm 1.0 \pm 0.4) \times 10^{-13}$	"	[97]
$\beta_{\oplus}(\tilde{\kappa}_{o+})^{YZ}$	$(-1.0 \pm 1.5) \times 10^{-17}$	"	[98]
$(\tilde{\kappa}_{o+})^{YZ}$	$(-2.8 \pm 2.2) \times 10^{-12}$	Optical, microwave resonators	[46]*
"	$(-3.2 \pm 2.3) \times 10^{-12}$	Rotating microwave resonators	[99]
"	$(2.9 \pm 2.8) \times 10^{-12}$	Rotating optical resonators	[100]
"	$(0.44 \pm 0.46) \times 10^{-11}$	Rotating microwave resonators	[101]
"	$(2.7 \pm 2.2) \times 10^{-11}$	Microwave resonator, maser	[102]
"	$(0.1 \pm 2.7) \times 10^{-11}$	Optical resonators	[103]

V. Alan Kostelecky & N. Russell:
Rev. Mod. Phys. 83, 11 (2011)
Data Tables for Lorentz and CPT violation
(latest version at arXiv:0801.0287v7)

コンプトン散乱

- 光子と電子が弾性散乱を起こし、光子のエネルギーの一部を電子に与える
- θ=180°のとき与えるエネルギーが最大
  →コンプトンエッジ(CE)

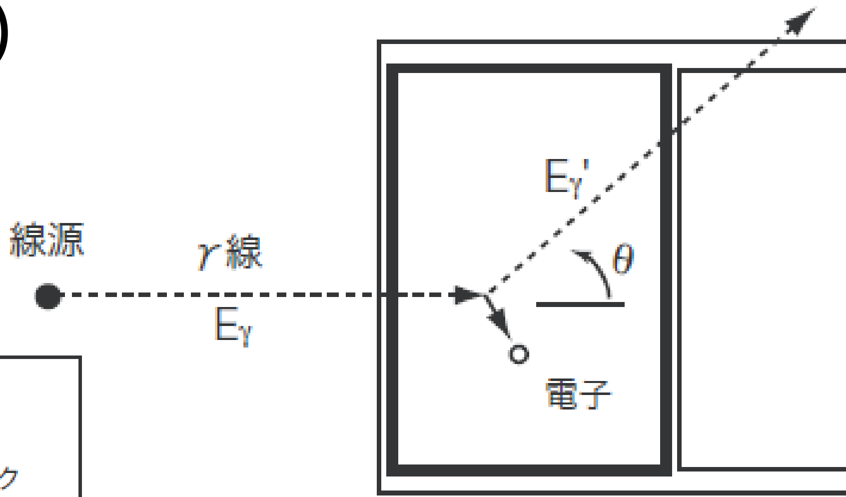

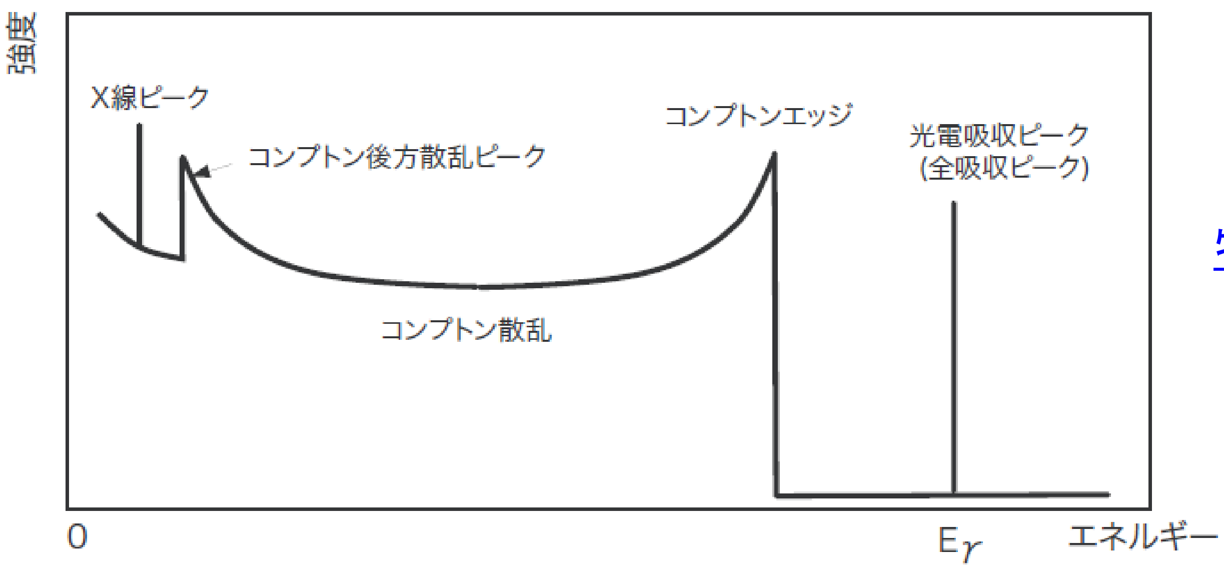

物理学実験I 解説書「放射線」より

コンプトンエッジが変わる

- 異方性があると光子の分散関係に異方性が出る

that the photon's dispersion relation is modified:

$$\omega = (1 - \vec{\kappa} \cdot \hat{\lambda})\lambda + \mathcal{O}(\kappa^2). \tag{1}$$

Here, $\lambda^\mu = (\omega, \lambda\hat{\lambda})$ denotes the photon four-momentum and $\hat{\lambda}$ is a unit three-vector. The three components of $\tilde{\kappa}_{0+}$

- CEエネルギーに異方性が出る

$$\lambda' \simeq \lambda_{\mathrm{CE}}\left[1 + \frac{2\gamma^2}{(1 + 4\gamma\lambda/m)^2}\vec{\kappa} \cdot \hat{p}\right]. \tag{3}$$

Here, $\lambda_{\mathrm{CE}} = \frac{4\gamma^2\lambda}{1+4\gamma\lambda/m}$ denotes the conventional value of the CE energy. Given the actual experimental data of $m =$

- 地球の自転に伴う変化量を見る

ESRF GRAAL Facility

- 欧州シンクロトロン放射光研究所
  (European Synchrotron Radiation Facility)
- GRenoble Anneau Accelerateur Laser
- Arレーザーが
  光子源(UV)
- 電子は6.03GeVに
  加速
- 1週間に渡って
  14765回
  スペクトル測定

上限値

- 得られた上限値

$$\Delta\lambda'/\lambda' < 2.5 \times 10^{-6} \quad (95\% \text{ C.L.}), \tag{8}$$

yielding the competitive limit $\sqrt{\kappa_X^2 + \kappa_Y^2} < 1.6 \times 10^{-14}$ (95% C.L.) with Eq. (4). Reinstating MSME notation and the electron coefficients for generality gives at 95% C.L.

$$\sqrt{[2c_{TX} - (\tilde{\kappa}_{0+})^{YZ}]^2 + [2c_{TY} - (\tilde{\kappa}_{0+})^{ZX}]^2} < 1.6 \times 10^{-14} \tag{9}$$

improving previous bounds by a factor of 10. The other, omitted MSME coefficients leave this limit unaffected.

- おそらくエネルギーの測定精度(統計誤差)で制限
- 磁場や位置は安定化されていて、電子の運動量は 10^{-6}レベル以上で安定化されているとしている

Quantum imaging

- G. B. Lemos et al.: Nature 512, 409 (2014)

LETTER

doi:10.1038/nature13586

Quantum imaging with undetected photons

Gabriela Barreto Lemos[1,2], Victoria Borish[1,3], Garrett D. Cole[2,3], Sven Ramelow[1,3]†, Radek Lapkiewicz[1,3] & Anton Zeilinger[1,2,3]

Information is central to quantum mechanics. In particular, quantum interference occurs only if there exists no information to distinguish between the superposed states. The mere possibility of obtaining information that could distinguish between overlapping states inhibits quantum interference[1,2]. Here we introduce and experimentally demonstrate a quantum imaging concept based on induced coherence without induced emission[3,4]. Our experiment uses two separate down-conversion nonlinear crystals (numbered NL1 and NL2), each illuminated by the same pump laser, creating one pair of photons

the signal single photon counts; the idlers are not detected. No coincidence detection is required.

The peculiar feature of this interferometer is that no detected photon has taken path d. Yet, in our experiment, it is precisely here where we put the object to be imaged. The key to this experiment is how the signal-source information carried by the undetected idler photon depends on T. For, if $T = 0$, an idler detected after D3, coincident with a signal count at $|g\rangle_s$ or $|h\rangle_s$, would imply the signal source was NL2. Detection of a signal photon without a coincident idler would imply the signal source

[1]Institute for Quantum Optics and Quantum Information, Austrian Academy of Sciences, Boltzmanngasse 3, Vienna A-1090, Austria. [2]Vienna Center for Quantum Science and Technology (VCQ), Faculty of Physics, University of Vienna, A-1090 Vienna, Austria. [3]Quantum Optics, Quantum Nanophysics, Quantum Information, University of Vienna, Boltzmanngasse 5, Vienna A-1090, Austria. †Present address: Cornell University, 159 Clark Hall, 142 Science Drive, Ithaca, New York 14853, USA.

実験装置概要

- 532nm(緑)を非線形光学結晶で810nm(黄)と1550nm(赤)に分ける
- NL1からの赤だけが見たいものを通るのに、NL1とNL2からの黄同士の干渉で見たいものが見える！

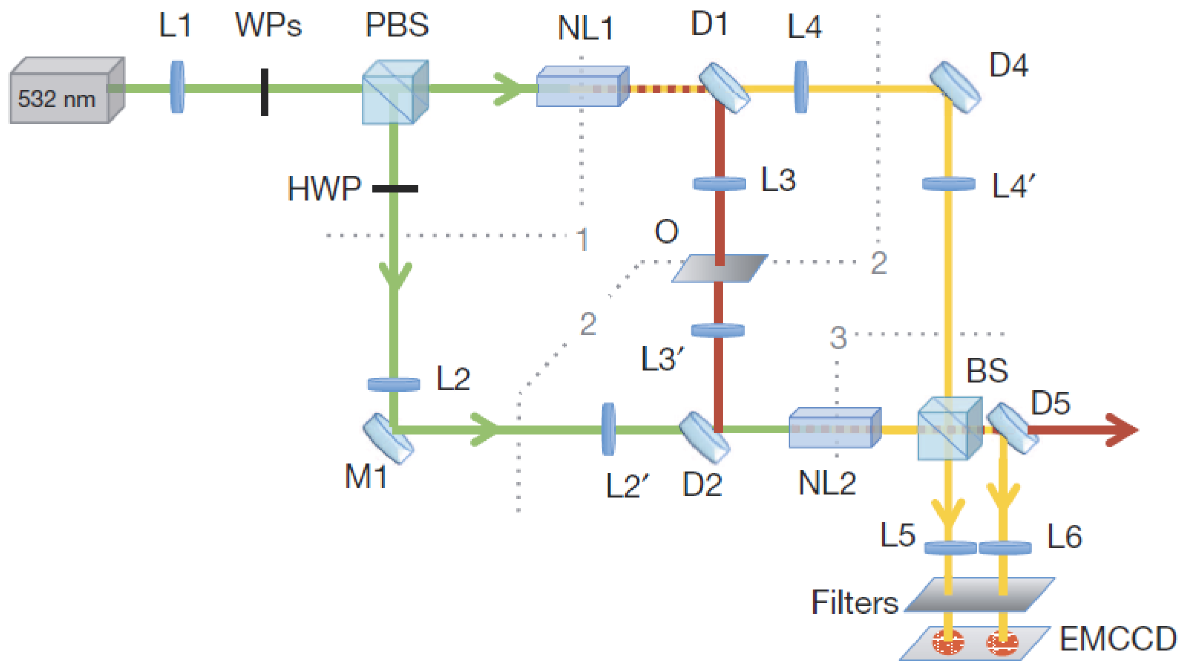

Figure 2 | Experimental set-up. A continuous-wave 532-nm laser (green) illuminates crystals NL1 and NL2. Wave plates (WPs) adjust the relative phase and intensity of the outputs of the polarizing beam splitter (PBS). The dichroic mirror D1 separates down-converted 810-nm (yellow) and 1,550-nm (red) photons. The 1,550-nm photons are transmitted through the object O and sent through NL2 by dichroic mirror D2. Lenses image plane 1 onto plane 3, and plane 2 onto the EMCCD camera. A 50:50 beam splitter (BS) combines the 810-nm beams. Dichroic mirrors D1, D2, D4 and D5 transmit the pump.

なぜか

- T=0の時、D3後の赤の検出で黄がNL1から来たのかNL2から来たのかわかってしまうので干渉が起きない
- T=1の時、赤の検出ではNL1かNL2か不明なので干渉が起こる(D2が重要ってこと！)
- interaction-free measurementと関連してる
  - Oに何もない時Ph=0とする
  - D3後の赤とhでの黄の同時検出でOにT=0のものがあるとわかる

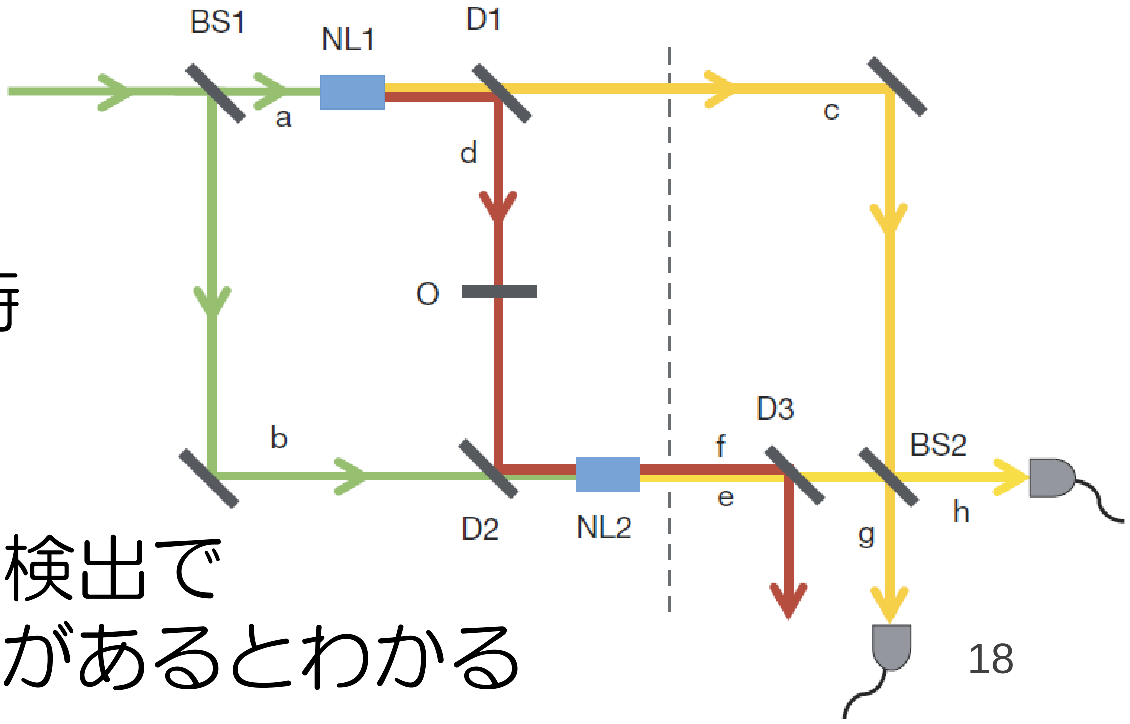

Kwiatらの実証実験

- P. Kwiat+: Ann. N. Y. Acad. Sci. 755, 383 (1995)
- P. Kwiat+: Phys. Rev. Lett. 74, 4763 (1995)

PHYSICAL REVIEW LETTERS

VOLUME 74 12 JUNE 1995 NUMBER 24

Interaction-Free Measurement

Paul Kwiat, Harald Weinfurter, Thomas Herzog, and Anton Zeilinger
Institut für Experimentalphysik, Universität Innsbruck, Technikerstrasse 25, 6020 Innsbruck, Austria

Mark A. Kasevich
Department of Physics, Stanford University, Stanford, California 94305
(Received 19 September 1994)

We show that one can ascertain the presence of an object in some sense without interacting with it. One repeatedly, but weakly, tests for the presence of the object, which would inhibit an otherwise coherent evolution of the interrogating photon. The fraction of "interaction-free" measurements can be arbitrarily close to 1. Using single photons in a Michelson interferometer, we have performed a preliminary demonstration of some of these ideas.

Kwiatらの実証実験

- 鏡で爆弾を模したMichelson干渉計
- “爆弾”を判別できる割合ηが理論と一致

Darkでの検出数
(鏡が入ったとわかった数)

$$\eta = \frac{P(\mathrm{det})}{P(\mathrm{det}) + P(\mathrm{abs})} = RT/(RT + R) = (1 - R)/(2 - R)$$

Objでの検出数
(爆発数)

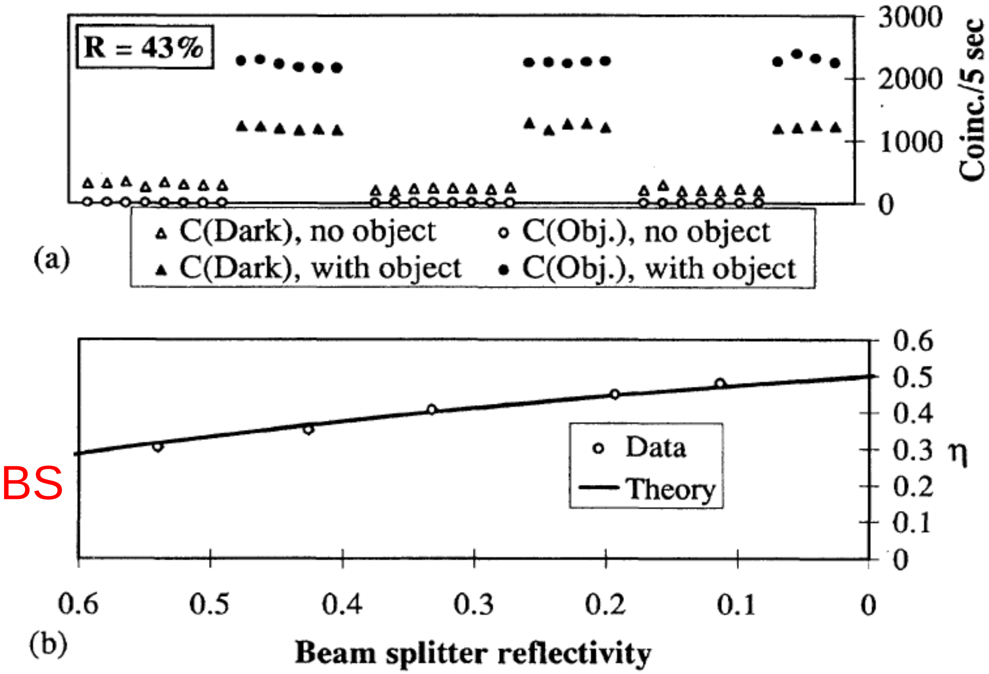

FIG. 5. (a) Typical experimental results for an interaction-free measurement. The beam splitter reflectivity for this data set was 43%. (b) Experimental and theoretical values for the figure of merit η in the Michelson-interferometer scheme, as a function of beam splitter reflectivity.

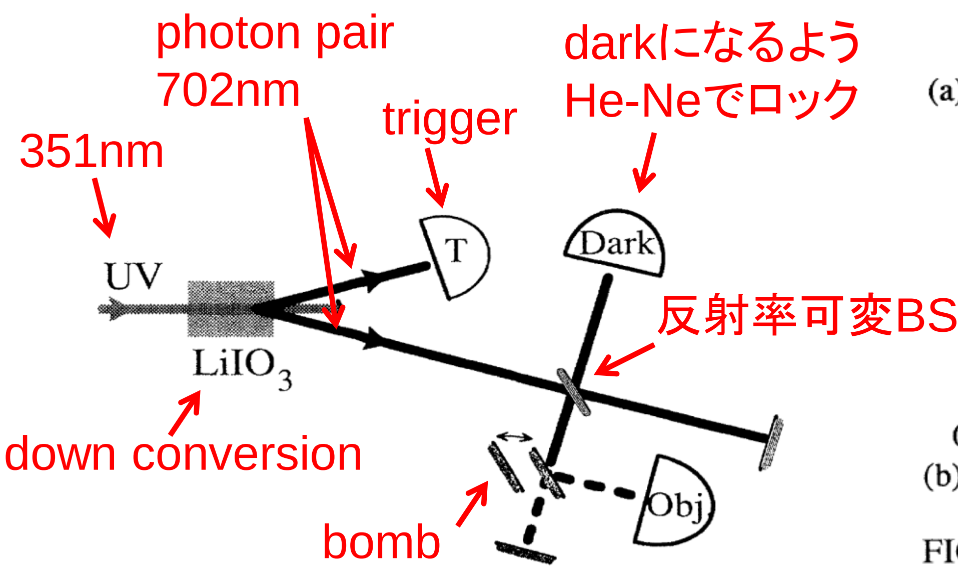

FIG. 4. Schematic of the down-conversion experiment demonstrating the principle of an interaction-free measurement.

デモ1

- T=0の部分では干渉が起きている (ちゃんとダークポートがある)
- T=1の部分では干渉が起きていない (光が半々になってるだけ)

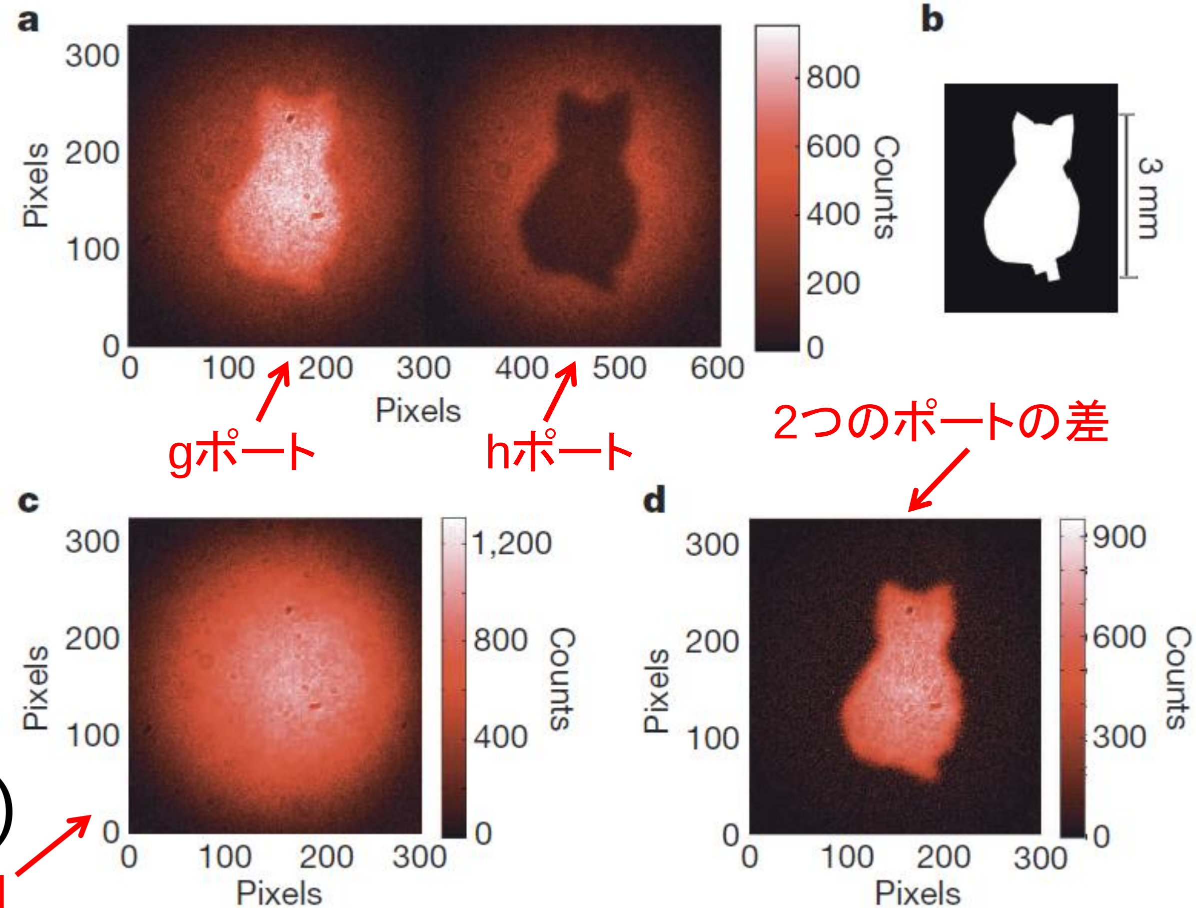

Figure 3 | Intensity imaging. **a**, Inside the cat, constructive and destructive interference are observed at the outputs of BS when we placed the cardboard cut-out shown in **b** in the path D1–D2. Outside the cat, idler photons from NL1 are blocked and therefore the signals do not interfere. **c**, The sum of the outputs gives the intensity profile of the signal beams. **d**, The subtraction of the outputs leads to an enhancement of the interference contrast, as it highlights the difference between constructive and destructive interference.

デモ2

- エッチングしたシリコンの板
- 赤には透明だが使った検出器は赤には不感
- 黄には不透明
- なのにちゃんと像が見えている
- 検出できないような光の波長でも試料を調べることができる！

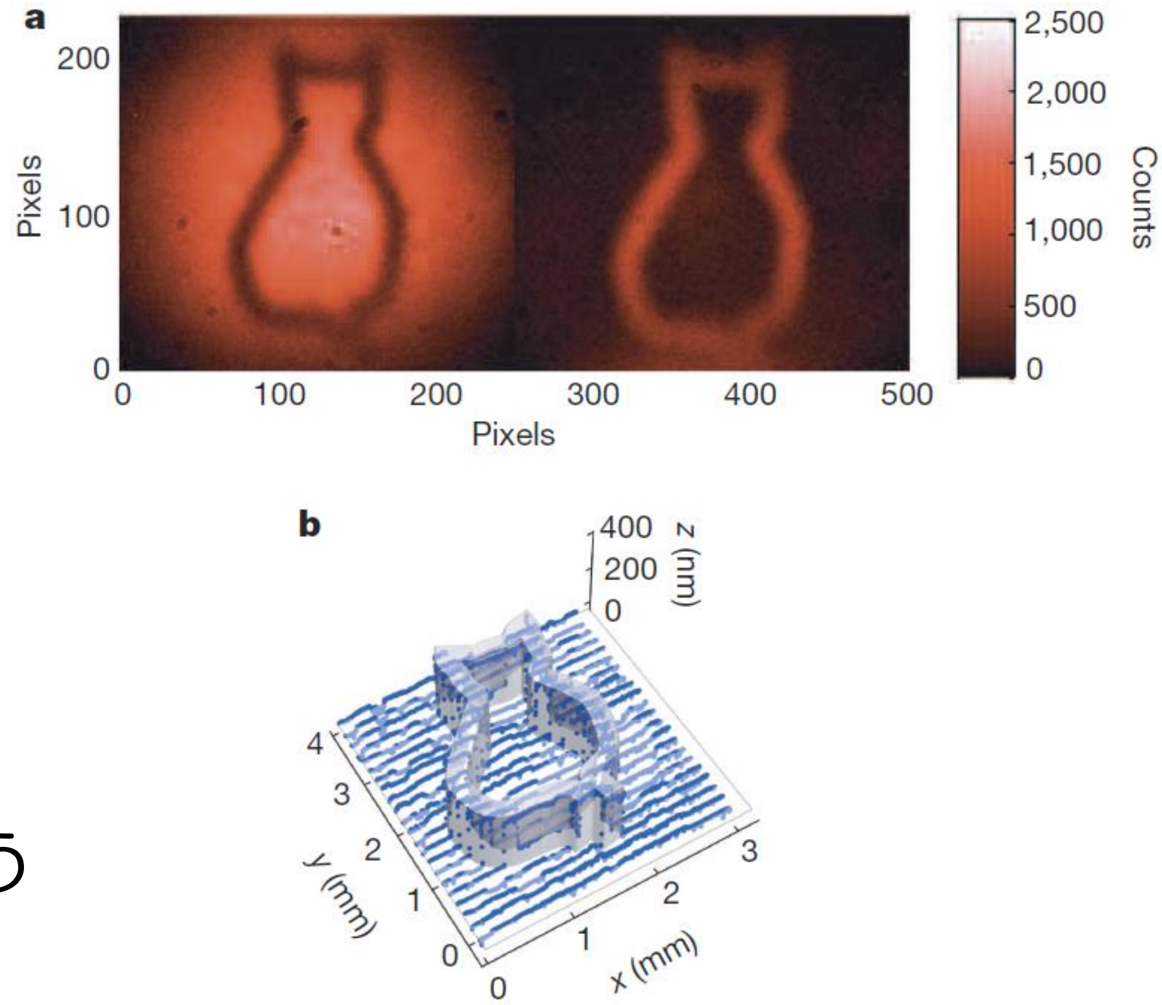

Figure 4 | Phase image of an object opaque to 810-nm light. a, Detection of 810-nm photons at both outputs of BS when a silicon plate (opaque to 810-nm light) with a 3-mm-tall etched cat (**b**) was introduced in path D1–D2. **b**, Three-dimensional rendering of the etch design overlaid with stylus profilometer scans (blue points) of the actual etch depth.

デモ3

- エッチングしたシリカの板
- 黄にとっては2π分の段差なので、黄側に入れても見えない(上)
- 赤にとってはπ分の段差なので干渉が見える(下)

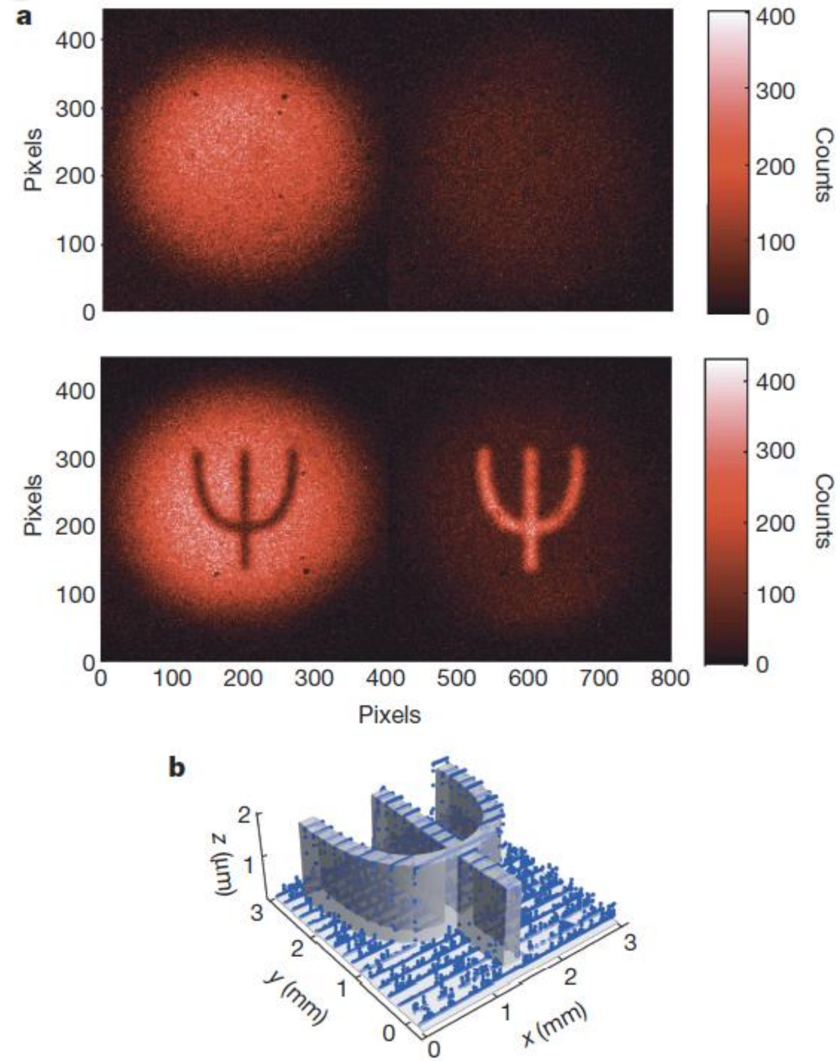

Figure 5 | Phase imaging of a 2π step at 820 nm. a, The top picture was taken with the object (shown in b) placed in the 820-nm beam between L4 and L4′; in the bottom picture, the object was placed in the 1,515-nm beam in path D1–D2. b, Three-dimensional rendering of the design overlaid with stylus profilometer scans (blue dots) of the actual etch depth.